1. Dominik DUDA[1], 2. Krzysztof MAŹNIEWSKI[1], 3. Bernard WITEK[1]

Silesian University of Technology, Faculty of Electrical Engineering, Department of Power System and Control (1)
ORCID: 1. 0000-0003-3247-2814; 2. 0000-0003-4357-6432, 3. 0000-0001-6732-9298

doi:10.15199/48.2023.05.12

Cable Inserts Modeling in Steady State Operating Conditions of High Voltage Networks.

***Abstract**. Selected problems occurring in high-voltage overhead-cable lines were analyzed. The Alternative Transients Program (ATP) environment was used to model and simulate the phenomena. Using the analytical relationships, the correctness of the model for analyzes in steady states was verified, and the waveforms of phase currents and voltages were examined. Among others, the influence of such factors as laying of HV cables in the trench, configuration of return conductors, use of ECC cable were analyzed. The obtained results confirm the correctness of the model, which during further investigations will be used the fault transient states analysis.*

***Streszczenie.** Przeanalizowano wybrane problemy występujące w napowietrzno-kablowych liniach wysokiego napięcia. Do symulacji i modelowania zjawisk wykorzystano środowisko Alternative Transients Program (ATP). Wykorzystując zależności analityczne zweryfikowano poprawność modelu do analiz w stanach ustalonych oraz zbadano przebiegi prądów i napięć fazowych. Przeanalizowano m.in. wpływ takich czynników jak, ułożenie kabli WN w wykopie, konfiguracja żył powrotnych, zastosowanie kabla ECC. Uzyskane wyniki potwierdzają poprawność modelu, który w dalszych badaniach zostanie wykorzystany do analizy nieustalonych stanów zwarciowych. (**Modelowanie wstawek kablowych w ustalonych stanach pracy sieci wysokiego napięcia**).*

Słowa kluczowe: napowietrzno-kablowe linie WN; model linii napowietrznej; model linii kablowej; Alternative Transients Program (ATP).
Keywords: HV overhead-cable lines; overhead line model; cable line model; Alternative Transients Program (ATP).

1. Introduction

High voltage (HV) overhead line sections must often be replaced by underground cable lines, due to the intersection of the line with various obstacles, including roads, rivers, buildings, or other power lines. In such an event, the cable insert must be selected such that its long-term and short-circuit load capacity is not less than the corresponding load capacity of the overhead line [1, 2]. These lines must also be protected against the effects of faults, and the protection must be properly parameterized. The model of the overhead cable line allows, among others to determine the trajectory of the phase-to-earth fault impedance phasors, and therefore may be applied for the correct parameterization of the distance protection. To minimize the modeling errors the model prepared in ATP should be verified. This issue is the main part of the article.

The impedances of the overhead part are determined by the parameters of the conductors and their geometrical layout as well as the parameters of the ground. In the case of a cable insertion, there are more factors on which impedances depend. These include: the structure of the cable, the arrangement of phase cables and their mutual spacing, the method of connecting and grounding the return conductors, grounding resistances at the transition from the overhead to the cable part, or additional elements of the cable line resulting from the method of connecting the return conductors. Therefore, this article mainly focuses on modeling the cable part of the power line.

In practice, two variants of cable arrangement are used for HV lines [4, 5]: trefoil formation and flat formation, with spacing between the cables. There are three ways of connecting and grounding the return wires: both-ends bonding (BE), single point bonding (SPB) and the cross bonding (CB). Due to large additional losses (power losses in cable return conductors), the BE system is the least frequently used system [5].

The SPB system is used for short lines, of up to approximately 1 km. However, this system requires the use of an additional earth continuity conductor (ECC) cable.

The ECC cable ensures a safe flow of single-phase short-circuit current in the event of a fault outside the cable line. Use of the cable substantially reduces the voltages induced across the return conductors. The unearthed ends of the return conductors should also be connected with appropriately selected sheath voltage limiters [6].

Use of the CB system is much more complex, but unavoidable in certain situations [6]; it is recommended for long cable lines and very high short-circuit currents. The system requires that the cable line is divided into 3*n* sections of the same length, where *n* is a natural number. By connecting the return conductor sections corresponding with successive phases of the cable line, a system is obtained for which the sum of induced voltages is zero. Consequently, no current flows through the return conductors during normal operation.

When considering the fault protection of HV networks, the cable line is often omitted or treated as a homogeneous element of the overhead line. However, such an approach may result in the incorrect operation of fault protections, and lead to thermal damage due to the flow of large currents of significant value [7, 8].

2. Power line modelling in the ATP

The literature describes many software environments that can produce mathematical models of power lines [9, 10]. Such models can be divided into those with lumped parameters and those with distributed parameters. Among other factors, this division concerns the relationships between specific conductivity γ, electric permeability ε, and magnetic permeability μ.

For the analysis of both *steady* and *transient* states phenomena within power lines, a model with distributed parameters is required. To begin, consider an elementary line segment of length Δ*x*, as shown in Fig. 1.

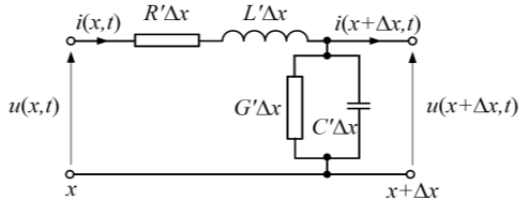

Fig. 1. Model of a power line segment [9].

Four quantities can be defined for each segment Δx: longitudinal resistance *R*, inductance *L*, shunt conductance *G*, and capacitance *C*. For the model shown Fig. 1, in

the limit that the length of the line segment goes to zero ($\Delta x \rightarrow 0$), if the considered line is homogeneous, we obtain:

(1a) $$\frac{\partial^2 u}{\partial x^2} = R'G'\ u + \left(R'C' + G'L'\right)\frac{\partial u}{\partial t} + L'C'\ \frac{\partial^2 u}{\partial t^2},$$

(1b) $$\frac{\partial^2 i}{\partial x^2} = R'G'\ i + \left(R'C' + G'L'\right)\frac{\partial i}{\partial t} + L'C'\ \frac{\partial^2 i}{\partial t^2}.$$

The mathematical (ATP) model of a HV cable is very well described in the references (e.g. [9, 10]). The EMTP programs offer various cable models for electromagnetic transients analysis – e.g. Bergeron/Dommel, J. Marti, L. Marti, Semlyen or Gustavsen. The advanced frequency-dependent (Semlyen) model of the single core cable which includes essential parameters of the cable elements and couplings, appropriate for the short circuit transients simulative analysis has been applied in the presented model.

In the frequency-dependent model, a line segment of length l between nodes "k" and "m" can be described by the system of equations

(2) $$\begin{bmatrix} U_{\mathrm{k}}(\omega) \\ I_{\mathrm{km}}(\omega) \end{bmatrix} = \begin{bmatrix} \cosh[\gamma(\omega)l] & Z_c \sinh[\gamma(\omega)l] \\ \frac{1}{Z_c}\sinh[\gamma(\omega)l] & \cosh[\gamma(\omega)l] \end{bmatrix} \begin{bmatrix} U_{\mathrm{m}}(\omega) \\ -I_{\mathrm{mk}}(\omega) \end{bmatrix}.$$

The parameters relevant for wave propagation in the line are the propagation coefficient and the characteristic impedance which can be written respectively

(3) $$\gamma = \sqrt{Y'(\omega)Z'(\omega)},$$

(4) $$Z_c = \sqrt{\frac{Z'(\omega)}{Y'(\omega)}}.$$

In this part of the paper only the steady states for model verification are concerned. To perform the transient state computations used for faults analysis describe in Part 2 , the equation (3) should be transformed into the time domain. For this purpose, the corresponding transformation is performed, during which, among others, a convolution integral is used. Detailed description of some mathematical models of overhead and cable lines can be found in [9, 10].

The assumed frequency range is of fundamental importance. The upper frequency limit should be chosen by taking into account the sampling frequency used for the calculation, which shows (according to Shannon's theorem) the maximum frequency of the reproduced signals. In practice, 1 MHz is recommended. The lower frequency limit is important for the initial value of the characteristic line impedance and the distribution of the zeroes/poles of the propagation function, which in turn affects the time constants of the models and extension of the steady state achievement at very low frequencies. From the practical experience [10, 11] it is recommended that the starting frequency is equal to 0.5 Hz and the number of zeroes and poles equals 20.

In order to ensure the symmetry of the line, it is also important to consider the phase transposing option.

2.1. Model of a HV power line with cable insert

Fig. 2 shows a general overview of a 110 kV network adopted for simulation tests. Equivalent systems SA and SB were modeled as ideal amplitude-and-phase-controlled voltage sources, allowing steady-state power flow. The 110 kV line connecting the two systems incorporated an 1 800 m cable segment. The overhead sections were 10 km long, and suspended from a typical B2 supporting structure. The ACSR phase conductors had a cross-section of 170 mm^2, and the ACSR lightning conductor had a cross-section of 95 mm^2. We modeled the cable section using the Cable LCC element from the ATP_Draw library (Fig. 3), based on the Semlyen model. The frequency-dependent Marti model was used for the overhead sections [9÷11]. The supply system S_A was defined as the protection point; the currents and voltages associated with line distance protection RZ_A were recorded from this point[1]. The influence of current and voltage transforms such as measurement errors or non-linear characteristics on the respective waveforms has been disregarded.

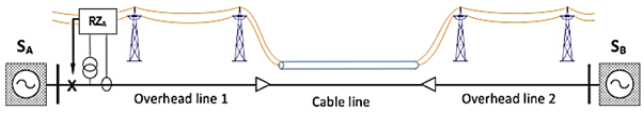

Fig 2. General overview of the overhead-cable line model.

We assumed that the modeled cable line was located underground at a depth of 1.3 m. Both flat and trefoil formations were investigated. For the flat formation, the distance between the axes of individual phase conductors was twice the diameter of the cables. For the trefoil formation, the cables were attached to a joint, so that the triangle tips were pointing upwards (see Fig. 3).

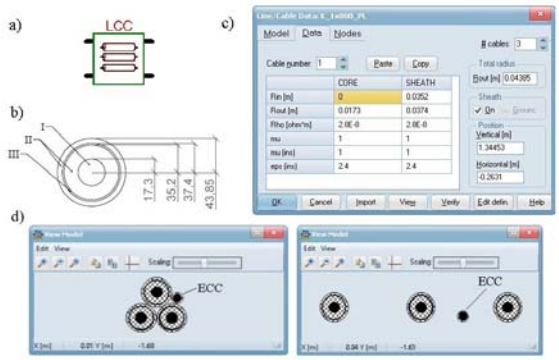

Fig. 3. Cable model in ATP_Draw, showing (a) the cable LCC module, (b) the cable XRUHKXS 1x800RM/95 mm^2 parameters (I - core, II - insulation, III - return conductor), (c) the cable LCC parameterization and (d) graphical representation of the SPB model, showing the trefoil formation and the flat formation.

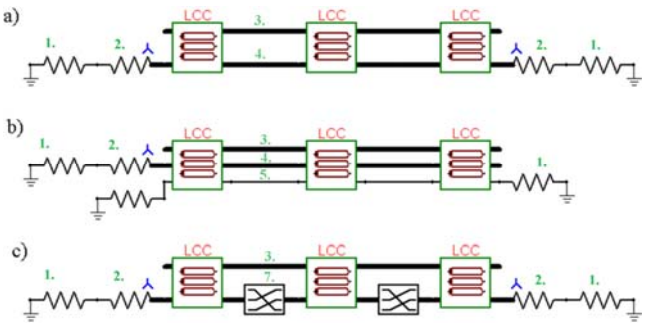

Fig. 4. Schemes of the cable (LCC) systems models in ATP_Draw: (a) BE system, (b) SPB system, (c) CB system; 1 – return cores earthing resistance (R_G = 5 Ω), 2 – star connected resistors system, low-impedance return cores connection with the ground, 3 – main conductor, 4 – return conductor, 5 – ECC, 7 – crossing box.

BE, CB, and SPB variants of the cable line were modeled. The configuration of the return conductors differed between each variant.

The cable layout was almost identical for the BE and CB configurations. The SPB configuration required the model to be expanded with an additional ECC cable to create a

[1] Analysis of faults and distance protection operation will be the subject of the authors' next article

return path for the earth fault current (see Fig. 3d and Fig. 4).

2.2. Verification of model correctness

BE system

In this configuration, the following phenomena occurred:
• significant, additional energy losses in the return conductors, particularly when using the flat formation;
• a voltage between the return conductors and earth of approximately zero (the reference earth in ATP model);
• in trefoil formation with symmetrical line load in the return conductors, induced currents of similar value, shifted relative to one another by 120° and 240°; and
• when using the flat formation, asymmetric currents and voltages induced in the return conductors [5, 6].

Fig. 5 shows examples of current waveforms in the cable return conductors, with a load current of 500 A. The flat cable formation produces noticeably greater asymmetry of phase currents and voltages than the trefoil formation. The currents flowing in the return conductors are less than half the size for the trefoil formation when compared to the flat formation.

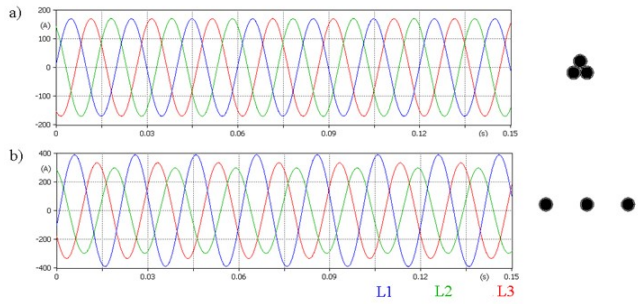

Figure 5. Current waveforms in the return conductors of the BE system in (a) trefoil and (b) flat formation.

When using the BE system, the root mean square (RMS) values of the I_s currents flowing in the HV cable return conductors can be determined analytically. By using the additional loss coefficients in the return conductors [6], and with a known current I flowing in the operating conductors,

$$\lambda = \frac{I_s^2 R_s}{I^2 R}, \tag{5}$$

where R_s is the AC resistance of the return conductor (Ω/km), and R is the AC resistance of the main conductor (Ω/km).

For the flat formation, without transposing individual cables, the outer cable carrying the lagging phase has the greatest loss. The additional loss factor for this cable is given by [3, 12]

$$\lambda_{11} = \frac{R_s}{R}\left[\frac{0{,}75P^2}{R_s^2+P^2} + \frac{0{,}25Q^2}{R_s^2+Q^2} + \frac{2R_s \cdot P \cdot Q \cdot X_m}{\sqrt{3}(R_s^2+P^2)\cdot(R_s^2+Q^2)}\right]. \tag{6}$$

Correspondingly, the additional loss factor of the other outer cable is given by

$$\lambda_{12} = \frac{R_s}{R}\left[\frac{0{,}75P^2}{R_s^2+P^2} + \frac{0{,}25Q^2}{R_s^2+Q^2} - \frac{2R_s \cdot P \cdot Q \cdot X_m}{\sqrt{3}(R_s^2+P^2)\cdot(R_s^2+Q^2)}\right]. \tag{7}$$

For the middle cable, the additional loss factor is given by

$$\lambda_{1m} = \frac{R_s}{R} \cdot \frac{Q^2}{R_s^2+Q^2}. \tag{8}$$

In Equations (4) and (5), we define:

$$P = X + X_m, \tag{9}$$

$$Q = X - \frac{X_m}{3}. \tag{10}$$

The reactance of the cable return conductors per unit length of cable for two adjacent single-core cables (Ω/km) is

$$X = 2\omega \cdot 10^{-4} \cdot \ln\left(\frac{2s}{d_s}\right), \tag{11}$$

where s is the axial distance between two adjacent single-core cables (m), and d_s is the mean diameter of the return conductor (m).

The mutual reactance per unit length of cable between the return conductor of an outer cable and the main conductors of the other two cables (Ω/km) is

$$X_m = 2\omega \cdot 10^{-4} \cdot \ln(2). \tag{12}$$

For the trefoil formation, the additional loss factor is the same for all cables, and can be analytically determined as

$$\lambda_1 = \frac{X^2}{R_s^2+X^2} \cdot \frac{R_s}{R}, \tag{13}$$

where X is given by Equation (11).

By combining Equation (5) with the additional loss factors of the return cables – given by Equations (6)÷(8) and Equation (13) for the flat formation and trefoil formation, respectively – we calculated the currents in the return cores of the L1-L3 cables using the following parameters:
• main conductor AC resistance R = 0,0358 Ω/km,
• return conductor R_s = 0,2373 Ω/km,
• axial distance between two adjacent single-core cables in flat formation s = 0.2631 m,
• axial distance between two adjacent single-core cables in trefoil formation s = 0.0877 m,
• return conductor mean diameter d_s = 0,0726 m.

Table 1. RMS and maximum current values and loss factors of the return conductors when using the BE system (λ - loss factor, I - load of cable line).

	flat formation				trefoil formation			
λ (–)	2.165		1.136		1.668		0.344	
I (A)	I_{sL1} (A)		I_{sL2} (A)		I_{sL3} (A)		I_{sL1-L3} (A)	
RMS	RMS	peak	RMS	peak	RMS	peak	RMS	peak
300	171.5	242.6	124.3	175.7	150.6	212.9	68.4	96.7
400	228.7	323.4	165.7	234.3	200.7	283.9	91.2	128.9
500	285.9	404.3	207.1	292.9	250.9	354.9	113.9	161.2
600	343.0	485.1	248.5	351.5	301.1	425.8	136.7	193.4

The calculation results are shown in Table 1. The line with a load of 500 A is indicated – the load for which the ATP simulation results are presented. The current values determined analytically are very similar to those obtained from simulation (as shown in Fig. 5).

The ground-relative voltage waveforms of the cable return conductors are similar for both the flat and trefoil formations. The waveforms exhibit a degree of asymmetry, and with a symmetrical load of 500 A on the main conductors, their peak values do not exceed 1 V.

CB system

In this configuration, the following phenomena occurred:
• non-zero voltages between the return conductors and the ground;
• very low currents induced in the cable return conductors, that did not affect the rating of the cables;
• asymmetry in the currents and voltages induced in the return conductors, when using the flat formation; and
• in the event of an earth fault, a significant voltage between the earth and the return wires [5, 6].

Fig. 6 shows the current and voltage waveforms in individual return cores when using the CB system in flat formation. For the trefoil formation, the current and ground-relative voltage waveforms of the return cores are

symmetrical. In trefoil formation the peak currents do not exceed 2 A, for a symmetric, linear and undistorted load of 500 A on the main conductors. The ground-relative return conductor voltages are much lower for the trefoil formation than for the flat formation.

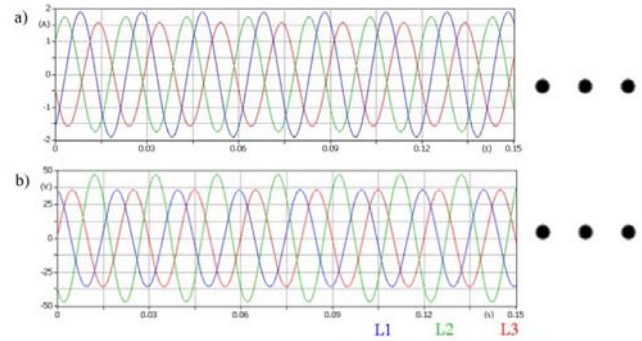

Fig. 6. The (a) current and (b) ground-relative voltage waveforms for the CB system in flat formation.

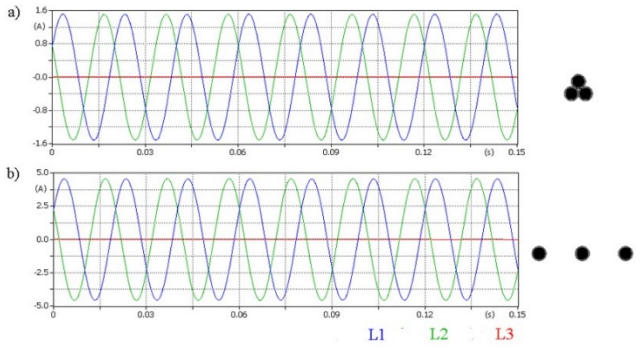

Fig. 7. Current waveforms in the return conductors when using the SPB system in (a) trefoil and (b) flat formation.

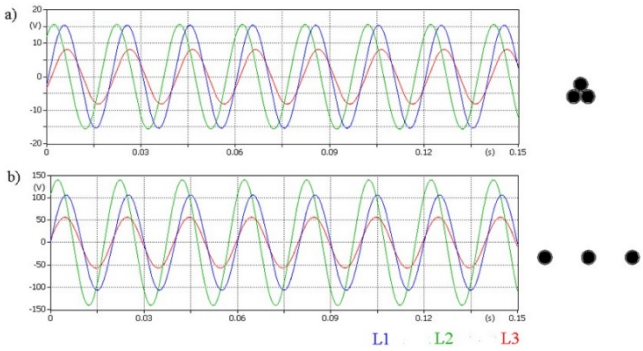

Fig. 8. Earth-relative voltage waveforms in the return conductors when using the SPB system in (a) trefoil and (b) flat formation. The localization of ECC was shown in Fig. 3.

SPB system

In this configuration, the following phenomena occurred:

• non-zero voltages between the return conductors and the ground;

• very low currents induced in the cable return conductors, that did not affect the capacity of the cables; and

• asymmetric currents and voltages induced in the return cores, due to the presence of an additional ECC cable, independent of the cable positioning within the trench [5, 6].

Figs. 7 and 8 show the current and voltage waveforms in the individual return cores. The current waveforms display noticeable asymmetry in both flat and trefoil formation. The L3 phase current is much lower than that of the other phases, due to the presence of an ECC cable that also induces current. The instantaneous voltages induced in the return conductors are significantly greater for the flat formation than for the trefoil formation. For both formations, the peak earth-relative voltage is significantly greater than that of the BE system. The instantaneous currents within the return conductors do not exceed 5 A, for a symmetric load of 500 A on the main conductors. This differs from the BE system due to the one-sided earthing of the return conductors.

3. Conclusions

Despite the recognition of the ATP program, the correctness of analyzes performed in this environment depends on correctly applied and parameterized models. The use of network element models requires verification before their proper application.

The obtained results show that the cable insertion model for the power frequency is compatible with the mathematical (analytical) models for the adequate methods of cable conductors laying and connecting and grounding their return conductors. This compliance is ensured, inter alia, by the correctness of impedance determination of the modeled cable insert in the fault conditions.

Protection algorithms (e.g. distance protection) are mainly based on the estimation of the fundamental current and voltage components, and then the impedance components for individual fault loops. This allows the conclusion that the developed model can also be used to simulate short-circuit conditions. Simulation tests may, inter alia, be used for the correct parameterization of the overhead and cable line protection, especially protection against the effects of earth faults. This issue will be the subject of a continuation of this article.

***Authors**: Department of Power System and Control, Faculty of Electrical Engineering, Silesian University of Technology, 44-100 Gliwice, Poland;*
Dominik Duda PhD, Eng, e-mail: dominik.duda@polsl.pl;
Krzysztof Maźniewski PhD, Eng., e-mail: krzysztof.mazniewski@polsl.pl; Bernard Witek PhD, Eng., Associate Prof., e-mail: bernard.witek@polsl.pl;

REFERENCES

[1] Anders G.J., Rating of Electric Power Cables in Unfavorable Thermal Environment; *John Wiley and Sons: Hoboken*, NJ, USA, 2005.
[2] Duda D., Long-term Ampacity of HV and MV Cable Lines; *Energetyka* 2021, 4, 329-338. (In Polish)
[3] Łowczowski K., Investigation of the influence of cable laying on energy losses in the return conductor - simulation in the PowerFactory program; *Przegląd Elektrotechniczny* 2016, 10, 54–57, doi:10.15199/48.2016.10.13
[4] CIGRE TB 531: Cable Systems Electrical Characteristics; WG B1.30, April 2013.
[5] CIGRE TB 797: Sheath Bonding Systems of AC Transmission Cables - Design, Testing, and Maintenance; WG.B1.50, March 2020.
[6] Żmuda K., Electrical Power Transmission and Distribution Systems; *Wydawnictwo Politechniki Śląskiej*, Gliwice, Poland, 2016. (In Polish)
[7] Witek B., Modeling of the Earth Faults in overhead – Cable HV Lines; *Energetyka* nr 2/2016, s. 99-104. (In Polish)
[8] Witek B., Some Aspects of Power System Protection in Cable and Overhead-Cable HV Lines; *Energetyka* nr 5/2016, s. 281-285.
[9] Rosołowski E., Computer Methods of Electromagnetic Transients Analysis. *Oficyna Wydawnicza Politechniki Wrocławskiej*, Wrocław 2009. (In Polish)
[10] Arrillaga J., Watson N.R., Computer Modeling of Electrical Power Systems; *Wiley & Sons*, Chichester 2001.
[11] Witek B., Selected issues of electrical power system computation and design. Vol. 1, Power transmission system; Gliwice, *Wydawnictwo Politechniki Śląskiej*, 2019.
[12] IEC 60287-1-1:2006 Electric cables - Calculation of the current rating - Part 1-1: Current rating equations (100% load factor) and calculation of losses – General, IEC: Geneva, Switzerland.